3

Accelerometers

Accelerometers are one of the highest volume MEMS products: The annual worldwide sales are more than 100 million units and are growing steadily. Historically, the automotive industry has been the growth driver. Today, all cars employ at least high-G crash sensors for air bag deployment. In addition, low-G sensors are used for active suspensions and vehicle stabilization controls. More recently, as the accelerometer prices have dropped to a dollar range, consumer applications have become economically feasible. For example, the latest generation of game consoles contains accelerometers for measuring the game controller movement to enable motion based user interface. Recently, cell phones enhanced with a motion based user interface have also become available. Accelerometers are also used by runners to determine the running speed and in digital cameras to determine the picture orientation. Some laptop hard drives utilize accelerometer based "free fall" detection to protect the hard drive from impacts. With the decreasing price, the number of accelerometer applications is going to increase in the coming years.

In this book, the accelerometers will be used to illustrate the microsensing techniques presented in later chapters. Chapter 4 covers the design of micromechanical springs used for the construction of microsensors. The piezoresistive and capacitive sensing principles are covered in detail in Chapters 5 and 6, respectively, and piezoelectric sensing is analyzed in Chapter 7. The interface electronics and the associated noise is covered in Chapter 8 and Chapter 9, respectively. Low switched capacitor circuits suitable for capacitive accelerometers are introduced in Chapter 10.

This chapter focuses on the fundamental principles of acceleration sensing. First, we will analyze the mechanical response of accelerometers. The response function is derived and studied in the frequency and time domain. After analyz-

ing the effect of damping and resonant frequency on the accelerometer response, we will cover the fundamental mechanical noise limitations. The chapter is concluded with case studies on surface and bulk micromachined accelerometers.

3.1 Operation principle

The accelerometer structure is illustrated in Figure 3.1. A proof mass m is connected to the frame by a flexible spring k. Due to the mass inertia, the proof mass motion will lag the frame motion. To prevent excessive ringing, the vibrations are damped by introducing gas (or liquid such as oil in macroscopic sensors) inside the package. This damping is represented with a dashpot γ.

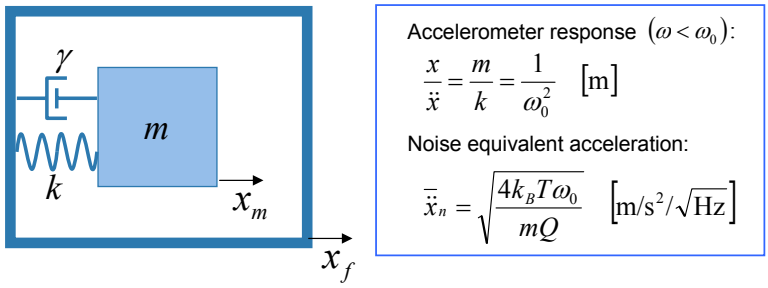

Figure 3.1: The basic structure of an accelerometer consists of a proof mass m that is suspended with a spring k to a frame. Due to inertia of the proof mass, the motion of the mass does not follow the frame motion and the difference in displacement $x = x_f - x_m$ can be used to measure the acceleration. Also provided is the noise-equivalent acceleration (due to mechanical Brownian noise).

The accelerometers can either be single axis or they can measure acceleration in multiple directions. In principle, a three axis accelerometer can be based on a single proof mass that can move in X-, Y-, and Z-directions. By measuring the mass displacement in all three directions, the acceleration can be deduced. Most practical sensors, however, measure the mass displacement along just one or two directions and multiple independent masses are used for three axis accelerometers [27].

The following sensing principles are used for micromechanical accelerometers [28]:

Piezoresistive sensing is based on piezoresistors integrated onto the spring. The piezoresistor resistance changes when subjected to the acceleration induced stress. Thus, by measuring the resistance change, the acceleration is deduced. The first micromachined silicon accelerometers developed in the 70's were based on piezoresistive sensing [29]. The piezoresistive sensing is robust and simple to implement but has poor noise and power performance. The piezoresistive sensing is covered in Chapter 5.

Capacitive sensing is based on detecting small change in capacitance due to relative movement of the proof mass and the frame. The capacitive accelerometers are currently the most widely used accelerometers as they are inexpensive, have good noise performance, and low power consumption. The capacitive sensing is covered in Chapter 6.

Piezoelectric sensing is based on a charge polarization of piezoelectric materials due to the strain caused by the inertial force. In the simplest configuration, the proof mass is attached to a piezoelectric plate that acts as a spring. The piezoelectric plate generates current that is proportional to the change in acceleration. As the sensor generates the current, the sensor is called self-generating. The drawback of piezoelectric sensors is that the sensor only measures the changes in acceleration and cannot be used to measure dc-acceleration. The piezoelectric sensing is commonly used for macroscopic sensors but is rarely used for microscopic accelerometers. The piezoelectric sensing is covered in Chapter 7.

In addition to the above sensing principles, optical and magnetic position detection have been used for macroscopic sensors [28], but these methods are not practical for microsensors.

3.2 Accelerometer equation

To analyze the accelerometer in Figure 3.1, we start with the equation of motion for the proof mass given by

$$m\frac{\partial^2 x_m}{\partial t^2} + \gamma\frac{\partial(x_m - x_f)}{\partial t} + k(x_m - x_f) = F_E, \tag{3.1}$$

where x_m and x_f are the positions of the mass and frame, respectively, and F_E is the external force acting on the mass for example due to actuation or Brownian noise. Equation (3.1) can be simplified by subtracting $m\frac{\partial^2 x_f}{\partial t^2}$ from both sides leading to

$$m\frac{\partial^2(x_m - x_f)}{\partial t^2} + \gamma\frac{\partial(x_m - x_f)}{\partial t} + k(x_m - x_f) = -m\frac{\partial^2 x_f}{\partial t^2} + F_e. \tag{3.2}$$

Recognizing that $x = x_f - x_m$ is the difference of the frame and mass positions leads to the familiar one degree-of-freedom damped resonator governed by

$$m\frac{\partial^2 x}{\partial t^2} + \gamma\frac{\partial x}{\partial t} + kx = F, \tag{3.3}$$

where F is the sum of inertial and external forces $F = m\frac{\partial^2 x_f}{\partial t^2} - F_E = m\ddot{x} - F_E$. Solving Equation (3.3) using Laplace transformation (see Appendixes A and B)

and defining the quality factor as $Q = \omega_0 m/\gamma$ gives

$$x = \frac{F/m}{s^2 + s\omega_0/Q + \omega_0^2} = \frac{\ddot{x}_f}{s^2 + s\omega_0/Q + \omega_0^2} \equiv H(s)\ddot{x}_f, \tag{3.4}$$

where we have assumed that there are no external forces ($F_E = 0$).

The frequency responses $H(s)$ for a critically damped accelerometer ($Q = 0.5$) as a function of the resonance frequency ω_0 are plotted in Figure 3.2. The low frequency response increases with the decreasing resonance frequency ω_0 and the high frequency displacement is seen as independent of the resonance frequency. Thus, reducing the resonant frequency increases the sensitivity but decreases -3 dB bandwidth.

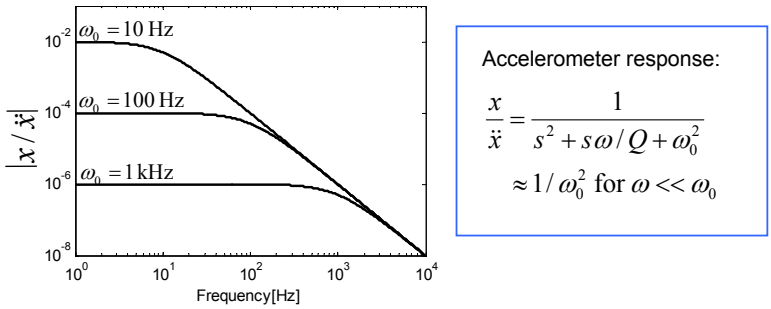

Figure 3.2: The frequency responses $x/\ddot{x} \equiv H(s)$ for a critically damped accelerometer ($Q = 0.5$).

3.2.1 Low-frequency response

The low-frequency response describes the accelerometer operation below its mechanical resonant frequency. Most MEMS sensors operate in this region with the typical resonant frequencies in the 10 Hz to 10 kHz range. From Equation (3.4), the low frequency response to acceleration $\ddot{x}$ is

$$x \approx m\ddot{x}_f/k = \ddot{x}_f/\omega_0^2 \quad \text{for} \quad \omega \ll \omega_0. \tag{3.5}$$

Equation (3.5) depends only on the resonance frequency suggesting that accelerometer size can be scaled without affecting the mechanical performance if the proof mass and spring constant are reduced proportionally. However, as was shown in Chapter 2, the mechanical vibrations due to thermal noise increase with decreasing mass size. As a result, large masses are desired for low noise sensors. The mechanical noise in accelerometers is further studied in Section 3.4.

Example 3.1: Accelerometer displacement
Problem: A capacitive accelerometer is to have a displacement of 0.5 μm at 2 G acceleration. Calculate the sensor resonant frequency.
Solution: From Equation (3.5) we obtain the resonant frequency as

$$f_0 = \frac{1}{2\pi}\sqrt{\left|\frac{\ddot{x}_f}{x}\right|} = \frac{1}{2\pi}\sqrt{\frac{2 \cdot 9.81 \text{ m/s}^2}{0.5 \ \mu\text{m}}} = 1.0 \text{ kHz}.$$

3.2.2 High-frequency response

Equation (3.5) shows that to obtain a sensitive accelerometer, the resonant frequency should be as low as possible. Taken to the extreme, the resonant frequency may be 1 Hz or lower and the sensor is operated above the natural frequency ($\omega \gg \omega_0$). These types of sensors are used as seismometers to measure the ground vibrations and earth quakes.

Substituting $\ddot{x}_f = s^2 x_f$ into Equation (3.4) and taking limit $\omega \gg \omega_0$ leads to

$$x \approx x_f \quad \text{for} \quad \omega \gg \omega_0. \tag{3.6}$$

The physical interpretation of Equation (3.6) is that at above resonance frequency, the proof mass essentially stays immobile and the difference of the mass and frame positions is simply $x = x_f - x_m \approx x_f$.

The mechanical resonance frequency of less than 1 Hz is obtainable with macroscopic devices that have large mass but is not easily achieved with small MEMS components. For this reason, the commercial MEMS accelerometers operate below the resonance frequency.

Example 3.2: A "MEMS seismometer" mass
Problem: A practical lower limit for a MEMS spring constant is around $k = 1$ N/m. Calculate the required proof mass dimensions to evaluate the feasibility of scaling down a macroscopic seismometer design with a resonant frequency of $f_0 = 0.2$ Hz.
Solution: With a spring constant $k = 1$ N/m, the required mass is

$$m = \frac{k}{\omega_0^2} \approx 0.63 \text{ kg}.$$

This corresponds to a cube of silicon with dimensions of

$$L = \left(\frac{m}{\rho}\right)^{1/3} \approx 6.5 \text{ cm},$$

which is not very micromechanical. If the resonance frequency was $f_0 = 100$ Hz, the mass would be $m = 2.5$ μkg and the size of mass would be 1 mm^3 – not quite micron-sized but typical for bulk micromachined accelerometers.

3.2.3 Time domain response

The time domain response is critical in many accelerometer applications. Ideally, the accelerometer output should follow the input (acceleration) instantaneously and without any error. However, as with any physical system, the accelerometer output will lag the change in acceleration. The mechanical response time is inversely related to the accelerometer resonance frequency ω_0. Moreover, the shape of the response depends on the damping: An under damped system shows significant overshoot and ringing and over damped systems are slow to respond. In commercial applications, a well-behaved response without ringing can be equally important as the fast response time. For example, in car stability control, under damping in the feedback control loop could result in oscillations with catastrophic consequences.

The step response describes the accelerometer response after a change in acceleration. The step response is studied systematically in Appendix B and we will summarize the results here. As shown in Figure 3.3, over damped accelerometers are slow to respond. Under damped devices are fast but the step response exhibits significant overshoot and ringing. The optimal speed is obtained with critical damping ($Q = 0.5$) that offers the fastest step response without overshoot or ringing.

In all cases, the displacement approaches the final displacement $x_{\text{final}} = F/k$. The transient error decays approximately as

$$err = |x - x_{\text{final}}| = e^{-t/\tau} \tag{3.7}$$

where τ is the time constant for the step response. From Appendix B, the time constant for under damped system ($Q > 0.5$) is $\tau_u = 2Q/\omega_0$ that describes how quickly the oscillations decay. For a critically damped ($Q = 0.5$) and over damped ($Q < 0.5$) systems, there is no closed form solution for the time constant. The settling times for the critical damped system are tabulated in Table B.1 on page 408. For over damped systems with $Q < 0.2$, the approximation $\tau_o \approx 1/\omega_0 Q$ can be used.

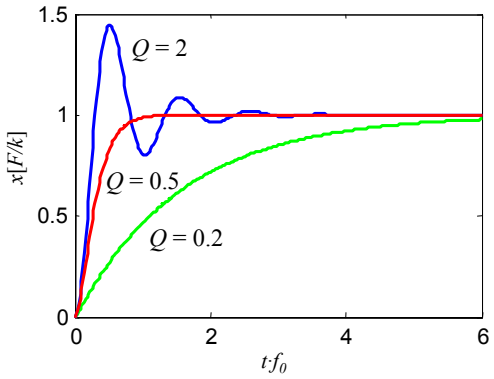

Figure 3.3: Accelerometer step responses for different quality factors (Figure B.2(c) from Appendix B reproduced here for convenience).

Example 3.3: Critically damped accelerometer settling time
Problem: A micromachined accelerometer has the resonant frequency $f_0 = 2.0$ kHz and the quality factor is $Q = 0.5$. How quickly does the accelerometer settle to within 1% of the final value?
Solution: For a critically damped system ($Q = 0.5$), the settling times are given in Table B.1 on page 408. The settling time to settle within 1% is

$$t_s = \frac{1.06}{f_0} \approx 0.5 \text{ ms}.$$

Example 3.4: Over damped accelerometer settling time
Problem: A micromachined accelerometer has the resonant frequency $f_0 = 2.0$ kHz and the quality factor is $Q = 0.1$. What is the time constant for the step response and how quickly does the accelerometer settle to within 1% of the final value?
Solution: For over damped critically damped system with $Q < 0.2$, the time constant is approximately

$$\tau \approx 1/\omega_0 Q \approx 80 \ \mu\text{s}.$$

Solving Equation (3.7) for $err = 0.01$ gives the time to settle to within 1% of the final value as

$$t = -\log(0.01)\tau \approx 4 \text{ ms},$$

which is almost ten times longer than for the critically damped accelerometer in Example 3.3.

3.3 Damping

The damping is controlled by the gas pressure inside the accelerometer package. The gas damping is covered in detail in Chapter 12 where the effect of device geometry and package pressure are analyzed. For now, it is sufficient to realize that the accelerometer damping can be adjusted with the device design. Often lowered package pressures are used to reduce the damping to an optimal level.

As shown in Figure 3.3, over damped accelerometers are slow to respond. Under damped devices are fast but the step response exhibits significant overshoot and ringing. The optimal speed is obtained with critical damping ($Q = 0.5$) that offers the fastest step response without overshoot or ringing.

Practical limitations in device design may cause the actual damping to be above or below the critical damping level. For example, real devices have multiple degrees of freedom and over damping may be used to suppress unwanted vibration modes and resonances. Here the response speed is traded for greater stability. Another extreme is the surface micromachined accelerometers that are under damped. The gas damping is less significant for laterally moving structures and surface micromachined accelerometers which can have $Q > 10$ even at atmospheric pressure. The high quality factor results in ringing of the proof mass that is not desired. To filter this ringing from the output signal, the bandwidth of the surface micromachined accelerometers is typically limited electrically to $\omega < \omega_0$.

Example 3.5: Damping coefficient
Problem: A micromachined accelerometer has the resonant frequency $f_0 = 2.0$ kHz and the mass $m = 0.5$ nkg. If the desired quality factor is $Q = 0.3$, what is the damping coefficient?
Solution: The damping coefficient is

$$\gamma = \frac{\omega_0 m}{Q} \approx 20.9 \ \mu\text{kg/s}.$$

3.4 Mechanical noise in accelerometers

The thermal noise induced mechanical vibrations set the lower limit for the measurable acceleration. In Chapter 2, we learned that noise force generator depends only on the dissipation and that small mechanical masses exhibit large noise induced vibrations.

For the noise analysis, it is helpful to model the mechanical system as a series connection of mass and spring as is shown in Figure 3.4. The mass m converts the acceleration into a force that is converted to a displacement by the spring k. The overall sensitivity $A = x/\ddot{x}$ is

$$A = A_1 A_2 = \frac{m}{k} = \frac{1}{\omega_0^2} \tag{3.8}$$

which is in agreement with Equation (3.5).

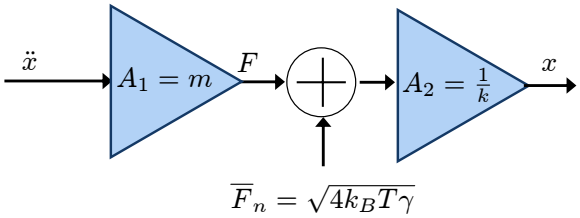

Figure 3.4: System level model for the accelerometer noise analysis.

The mechanical noise is modeled by the mechanical noise force generator $\overline{F}_n = \sqrt{4k_BT\gamma}$. As shown in Section 2.5, the input referred noise can be used to quantify the sensor noise performance as it gives a direct measure of the smallest measurable acceleration. The input referred noise equivalent acceleration spectral density is

$$\overline{\ddot{x}}_n = \frac{\overline{F}_n}{A_1} = \frac{\overline{F}_n}{m} = \frac{\sqrt{4k_BT\gamma}}{m} = \sqrt{\frac{4k_BT\omega_0}{mQ}}. \tag{3.9}$$

The noise equivalent acceleration given by Equation (3.9) is a measure of the smallest acceleration that can be measured: Acceleration smaller than $\overline{\ddot{x}}_n$ generate displacement that is below the thermal noise floor $\overline{x}_n$ for the mechanical vibrations.

Equation (3.9) suggests that the noise could be reduced by increasing the quality factor, increasing the mass, and reducing the resonant frequency ω_0. However, the benefit of increasing the quality factor is purely superficial. From the equipartition theorem, we know that the total noise energy integrated

over all frequencies is constant. The rms-vibration amplitude given by Equation (2.24) is $x_{\text{rms}} = \sqrt{\frac{k_B T}{k}}$, which is independent of quality factor. Given the rms-displacement, the input referred rms-acceleration is

$$\ddot{x}_{\text{rms}} = \frac{x_{\text{rms}}}{A_1 A_2} = x_{\text{rms}} \omega_0^2 = \sqrt{\frac{\omega_0^2 k_B T}{m}}. \tag{3.10}$$

Equation (3.10) clearly shows that the quality factor does not affect the total input referred acceleration noise. In addition, the high-Q has the detrimental effect of increasing the step response time. Thus, increasing the proof mass and lowering the resonant frequency are the only effective methods to reduce the mechanical noise. This partially explains why there are no "nanomechanical" accelerometers on market.

Example 3.6: Accelerometer noise
Problem: A MEMS accelerometer has the mass $m = 0.5$ nkg and the mechanical resonant frequency $f_0 = 2$ kHz. Calculate the proof mass rms-noise displacement and the input referred rms-noise equivalent acceleration.
Solution: The element spring constant is $k = \omega_0^2 m = 12.67$ N/m and the rms-displacement due to thermal noise from Equation (2.24) is

$$x_{\text{rms}} = \sqrt{\frac{k_B T}{k}} \approx 2.3 \cdot 10^{-10} \text{ m}.$$

From Equation (3.10), the input referred noise equivalent acceleration is

$$\ddot{x}_{\text{rms}} = x_{\text{rms}} \omega_0^2 \approx 0.0362 \text{m/s}^2 = 3.7 \text{ mG}.$$

Example 3.7: A Silicon accelerometer
Problem: Figure 3.5 shows a schematic of a bulk micromachined accelerometer. The mass dimensions are 1200 μm $\times$ 1200 μm $\times$ 550 μm and the silicon density is 2330 kg/m^3. The total spring constant for the four beams is $k = 40$ N/m and targeted quality factor is $Q = 0.2$. What is the
a) sensor resonance frequency?
b) damping coefficient?
c) proof mass displacement due to 1 G acceleration at low frequencies

($\omega \ll \omega_0$)?
d) noise induced displacement spectral density at low frequencies ($\omega \ll \omega_0$)?
e) proof mass rms-displacement due to noise?
f) noise equivalent acceleration (the spectral density and rms-noise)?

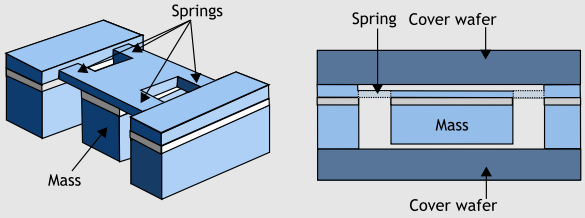

Figure 3.5: Silicon micromachined accelerometer. The proof mass displacement could be detected piezoresistively or capacitively.

Solution: a) The mass is $m = \rho V = 1.845$ μkg and the resonance frequency is $f_0 = \frac{1}{2\pi}\sqrt{\frac{k}{m}} = 737.7$ Hz$\approx$ 740 Hz.
b) The damping coefficient is $\gamma = \frac{m\omega_0}{Q} = 0.0428$ μkg/s ≈ 0.043 μkg/s.
c) The proof mass displacement due to the 1-G acceleration is $x = \ddot{x}/\omega_0^2 = 0.4565$ μm ≈ 0.46 μm.
d) The noise induced displacement spectral density is

$$\bar{x}_n = \sqrt{\bar{x_n^2}} = \frac{F_n}{k} = \frac{\sqrt{4k_BT\gamma}}{k} \approx 0.67 \cdot 10^{-12} \text{ m}/\sqrt{\text{Hz}}$$

e) The equipartition theorem states that the average potential energy due to thermal noise is $W = \frac{1}{2}k_BT$. Writing $W = \frac{1}{2}kx_{\text{rms}}^2 = \frac{1}{2}k_BT$ gives

$$x_{\text{rms}} = \sqrt{\frac{k_BT}{k}} = 10.22 \text{ pm} \approx 10 \text{ pm}.$$

f) The equivalent acceleration noise spectral density from Equation (3.9)is

$$\bar{\ddot{x}}_n = \sqrt{\frac{4k_BT\omega_0}{mQ}} = 1.44 \cdot 10^{-5} \text{ m/s}^2/\sqrt{\text{Hz}} \approx 1.47 \ \mu\text{G}/\sqrt{\text{Hz}}.$$

and the rms-noise from Equation (3.10) is

$$\ddot{x}_{\text{rms}} = \sqrt{\frac{\omega_0^2 k_BT}{m}} \approx 0.22 \text{ m/s}^2 \approx 22 \ \mu\text{G}.$$

3.5 Commercial devices

To exemplify what we have learned, we will analyze two commercial micromechanical accelerometers. The first device is a surface micromachined accelerometer that has a relatively small mass. The second device is a bulk micromachined accelerometer that has 10^4 times larger mass. By comparing the intrinsic noise for the two accelerometers, it is clear that a large mass is needed for low noise. The low intrinsic noise however, does not guarantee low overall noise. For the analyzed devices, the overall sensor noise performance including the noise from circuitry is an order of magnitude worse than the mechanical noise limit.

3.5.1 Case study: A surface micromachined accelerometer

Figure 3.6 shows a schematic for a surface micromachined accelerometer. The structure and design parameters are similar to ADXL50 accelerometer from Analog Devices [30–32]. The proof mass is suspended by folded spring beams and moves in plane above the die surface. The proof mass motion relative to the substrate is measured with fixed sensing fingers that are anchored to the substrate. The capacitance measurement sensitivity is increased by measuring the differential capacitance change $C_1 - C_2$ between two electrodes. The differential capacitive measurement is analyzed in detail in Chapter 6.

As the sensing element is relatively thin ($\sim$2 μm), several sensing fingers are combined in parallel to increase the overall capacitance. Typical surface micromachine designs have 40-100 finger pairs but for illustrative purposes only 6 pairs are shown. Using the element values in Figure 3.6 and Equations (3.5) and (3.9) we obtain $x/\ddot{x} = 0.4$ nm/G and $\overline{\ddot{x}}_n = 0.2$ mG/$\sqrt{\text{Hz}}$ for the element sensitivity and noise, respectively. The intrinsic noise can be compared to noise performance specifications of $\overline{\ddot{x}}_n = 1$ mG/$\sqrt{\text{Hz}}$ in manufacturer's data sheets [30]. The total noise including the measuring circuitry is a factor five higher that the mechanical noise alone.

3.5.2 Case study: A bulk micromachined accelerometer

A typical bulk micromachined accelerometer is shown in Figure 3.7. The proof mass moves in Z-direction in response to the Z-axis acceleration. The mass displacement is detected by measuring the differential capacitance changes between the proof mass and the top and bottom electrodes.

Representative device dimensions for a bulk micromachined accelerometer are 1 mm×1 mm×0.38 mm. The mass and spring constant are $1 \cdot 10^{-6}$ kg and 50 N/m, respectively. Using Equations (3.5) and (3.9), we obtain $x/\ddot{x} = 0.2$ μm/G and $\overline{\ddot{x}}_n = 3$ μG/$\sqrt{\text{Hz}}$ for the element sensitivity and noise, respectively. The intrinsic noise can be compared to the noise performance specifications of $\overline{\ddot{x}}_n = 20$ μG/$\sqrt{\text{Hz}}$ for a commercial accelerometer (SCA620 from

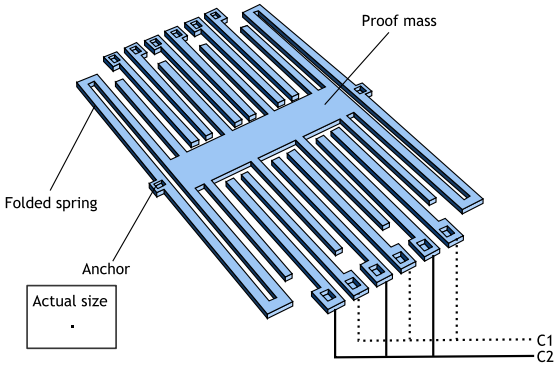

Parameter	Value	Units
Resonant frequency, f_0	25	kHz
Mass, m	0.2	nkg
Spring constant, k	5	N/m
Sense capacitance, C_0	0.1	pF
Quality factor, Q	5	

(a) A surface micromachined accelerometer and typical element parameters corresponding to ADXL50 accelerometer from Analog Devices.

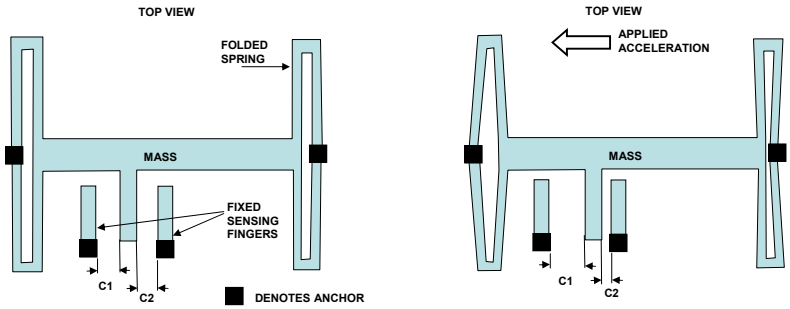

(b) The movement of the proof mass is detected by measuring the capacitance change between proof mass fingers and fixed sensing fingers. Typical designs have 40-100 finger pairs to increase total capacitance.

Figure 3.6: A schematic of typical surface micromachined accelerometer (After Analog Devices data sheet [30]).

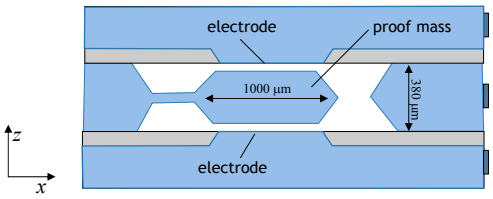

Parameter	Value	Units
Resonant frequency, f_0	1	kHz
Mass, m	1	μkg
Spring constant, k	50	N/m
Sense capacitance, C_0	5	pF
Quality factor, Q	0.1	

Figure 3.7: A bulk micromachined accelerometer and typical element parameters.

VTI Technologies [33]). We see that when noise from the measuring circuitry is included, the total noise is a factor of eight larger than the mechanical noise limit.

When comparing the surface and bulk micromachined accelerometers, it is evident that the large mass of the bulk micromachined device enables lower noise. In addition, the bulk micromachined accelerometer has a large sensitivity which further increases signal-to-noise ratio. This need for high sensitivity will be further investigated in Chapter 9 where the circuit noise is analyzed.

Key concepts

- Accelerometers consist of a proof mass and a spring. By measuring the proof mass displacement relative to the frame, the acceleration can be deduced.
- At low-frequencies ($\omega \ll \omega_0$), the inertial force $F = m\ddot{x}$ is balanced by the spring force $F = kx$. The accelerometer response $x/\ddot{x} = m/k = 1/\omega_0^2$ is inversely proportional to the resonance frequency squared.
- The mechanical noise sets the limit for the acceleration noise floor.
- The input referred noise equivalent acceleration spectral density is $\overline{\ddot{x}}_n = \frac{\overline{F}_n}{m} = \sqrt{\frac{4k_BT\omega_0}{mQ}}$.
- The input referred noise equivalent rms-acceleration is $\ddot{x}_{\text{rms}} = \sqrt{\frac{\omega_0^2 k_B T}{m}}$.
- The system noise performance depends on both mechanical and electrical noise. In commercial devices, the electrical noise is typically larger than the fundamental mechanical noise limit.

Exercises

Exercise 3.1
Using your favorite search engine, find at least five MEMS accelerometer manufacturers.

Exercise 3.2
Calculate how big mass would be needed to obtain mechanical noise limit of $\ddot{x}_{\text{rms}} = 1$ nG, 1 μG, and 1 mG if the mechanical resonance frequency is 100 Hz. If the mass is made of silicon, what would its physical dimensions be?

Exercise 3.3
Explain how the quality factor Q and the resonance frequency f_0 affect the accelerometer settling time.

Exercise 3.4
A capacitive accelerometer with 50 G full-scale acceleration is to have a maximum displacement of 1.5 μm. What is the lowest possible resonant frequency for the accelerometer?

Exercise 3.5
A micromachined accelerometer has the resonant frequency $f_0 = 100$ Hz and the quality factor is $Q = 0.2$. What is the time constant for the step response and how quickly the accelerometer settles to within 5% of the final value?

Exercise 3.6
A micromachined accelerometer has the resonant frequency $f_0 = 100$ Hz and the mass $m = 0.4$ μkg. If the desired quality factor is $Q = 0.2$, what is the damping coefficient?

Exercise 3.7
Consider the commercial accelerometer in Figure 3.7. What is the smallest proof mass size that could would lead to mechanical noise equal to the noise performance specifications of $\overline{\ddot{x}}_n = 20$ $\mu\text{G}/\sqrt{\text{Hz}}$ in manufacturers data sheet? Assume that the resonant frequency is constant ($f_0 = 1$ kHz). Compare your results to the estimated actual mass $m = 1$ μkg.

Exercise 3.8
The low-G accelerometer ADXL05 from Analog Devices has a pm5-G full scale range and the noise floor is 500 $\mu\text{G}/\sqrt{\text{Hz}}$ (12$\times$ less than ADXL50). Assume that the characteristics of ADXL05 are identical to those given in Figure 3.6 except for $k = 0.4$ N/m and $f_0 = 10$ kHz. Calculate the intrinsic acceleration noise spectral density and sensor element sensitivity (displacement for a 1-G acceleration). Compare numbers to ADXL50 in Figure 3.6.

Exercise 3.9
In this problem you are to explore noise in a micromachined accelerometer. Figure 3.8 shows an accelerometer fabricated of SOI (silicon on insulator) wafer. The plate dimensions are 200 μm $\times$ 200 μm $\times$ 10 μm and the silicon density is 2330 kg/m^3. The spring constant is $k = 0.08$ N/m and damping coefficient due viscous air damping is $\gamma = 4$ μkg/s. What is the
a) sensor resonance frequency?
b) noise induced displacement spectral density below the resonance frequency?
c) proof mass rms-displacement due to noise?
d) noise equivalent acceleration spectral density?
e) How should the sensor be modified to obtain noise floor of 1 $\mu\text{G}/\sqrt{\text{Hz}}$ if bandwidth is to remain constant?

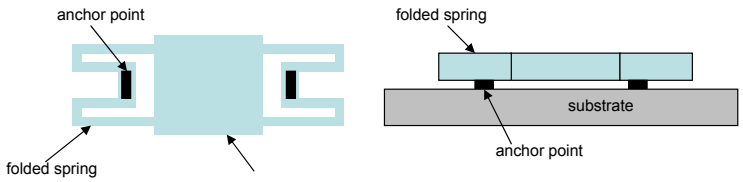

Figure 3.8: Figure for Exercise 3.9. A schematic view of SOI accelerometer (Left: top view, Right: side view).

Exercise 3.10

Figure 3.9 shows how the total output noise can be reduced electronically with a low pass filter. Although the total mechanical rms-noise is constant, we can limit the mechanical noise at the electronics output by increasing quality factor Q and low pass filtering the measured signal. After filtering, the total rms-noise is $\ddot{x}_{\text{rms}} = \overline{\ddot{x}_n}\sqrt{BW}$, where BW is the filter bandwisth. Investigate whether this is a viable method make an accelerometer with performance "beyond noise floor" (total noise less than the rms-noise given by Equation (3.10)). Hint: take the sensitivity, the total thermal noise, and the settling time as the critical parameters. Compare of the noise shaped accelerometer to that of critically damped accelerometer that has same mass but smaller resonance frequency corresponding to bandwidth of the filtered accelerometer. Are there other factors that should be considered for fair judgment between the merits of electrical vs. mechanical bandwidth limiting?

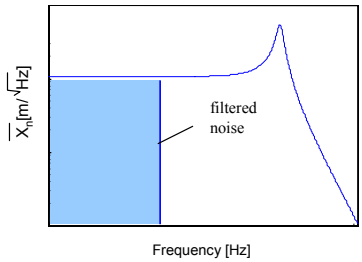

Figure 3.9: Figure for Excercise 3.10. The mechanical noise is electrically filtered so that the total measured rms-noise is less than $x_{\text{rms}} = \sqrt{\frac{k_B T}{k}}$.